




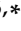





Article

Isolation of Arborescin from *Artemisia absinthium* L. and Study of Its Antioxidant and Antimicrobial Potential by Use of In Vitro and In Silico Approaches

Asmae Hbika ^{1,*}, Amine Elbouzidi ^{2,3}, Mohamed Taibi ^{2,4}, Safae Ouahabi ¹, El Hassania Loukili ³, Abdelhamid Bouyanzer ¹, Meryem Idrissi Yahyaoui ⁵, Abdeslam Asehraou ⁵, Naoufal El Hachlafi ^{6,*}, Ahmad Mohammad Salamatullah ⁷, Mohammed Bourhia ⁸, Samir Ibenmoussa ⁹, Mohamed Addi ², and Elkhadir Gharibi ^{10,*}

- ¹ Laboratory of Applied and Environmental Chemistry (LCAE), Team Applied Analytical Chemistry of Materials, Mohammed First University, Oujda 60000, Morocco; safaeouahabi86@gmail.com (S.O.); bouyanzer@yahoo.fr (A.B.)
 - ² Laboratory for Agricultural Productions Improvement, Biotechnology and Environment (LAPABE), Faculty of Sciences, University of Mohammed First, Oujda 60000, Morocco; amine.elbouzidi@ump.ac.ma (A.E.); mohamedtaibi9@hotmail.fr (M.T.); m.addi@ump.ac.ma (M.A.)
 - ³ Euromed University of Fes, UEMF, Fes 30000, Morocco; hassania-loukili@hotmail.com
 - ⁴ Center of Oriental Water and Environmental Sciences and Technologies (COSTEE), University of Mohammed First, Oujda 60000, Morocco
 - ⁵ Laboratory of Bioresources, Biotechnology, Ethnopharmacology and Health, Faculty of Sciences, Mohammed First University, Boulevard Mohamed VI, Oujda 60000, Morocco; iy.meryem@ump.ac.ma (M.I.Y.); asehraou@gmail.com (A.A.)
 - ⁶ Laboratory of Microbial Biotechnology and Bioactive Molecules, Faculty of Sciences and Technologies, Sidi Mohamed Ben Abdellah University, Imouzzer Road, P.O. Box 2202, Fez 30000, Morocco
 - ⁷ Department of Food Science & Nutrition, College of Food and Agricultural Sciences, King Saud University, P.O. Box 2460, Riyadh 11451, Saudi Arabia; asalamh@ksu.edu.sa
 - ⁸ Laboratory of Biotechnology and Natural Resources Valorization, Faculty of Sciences, Ibn Zohr University, Agadir 80060, Morocco; m.bourhia@uiz.ac.ma
 - ⁹ Laboratory of Therapeutic and Organic Chemistry, Faculty of Pharmacy, University of Montpellier, 34000 Montpellier, France; ibenmoussa@yahoo.fr
 - ¹⁰ Laboratory of Applied and Environmental Chemistry (LCAE), Team Solid Mineral Chemistry, University of Mohammed First, Oujda 60000, Morocco
- * Correspondence: asmae.hbika@gmail.com (A.H.); naoufal.elhachlafi@usmba.ac.ma (N.E.H.); gharibi_elkhadir@yahoo.fr (E.G.)



Citation: Hbika, A.; Elbouzidi, A.; Taibi, M.; Ouahabi, S.; Loukili, E.H.; Bouyanzer, A.; Yahyaoui, M.I.; Asehraou, A.; El Hachlafi, N.; Salamatullah, A.M.; et al. Isolation of Arborescin from *Artemisia absinthium* L. and Study of Its Antioxidant and Antimicrobial Potential by Use of In Vitro and In Silico Approaches.

Separations **2024**, *11*, 209.
<https://doi.org/10.3390/separations11070209>

Academic Editor: Léon Reubsæet

Received: 22 May 2024
Revised: 23 June 2024
Accepted: 26 June 2024
Published: 5 July 2024



Copyright: © 2024 by the authors. Licensee MDPI, Basel, Switzerland. This article is an open access article distributed under the terms and conditions of the Creative Commons Attribution (CC BY) license (<https://creativecommons.org/licenses/by/4.0/>).

Abstract: This study focused on developing an innovative, straightforward, and economical method utilizing a mixture of readily available solvents to extract arborescin (C₂OH₂OO₈) crystals from *Artemisia absinthium* L. (*A. absinthium*). The structural elucidation and characterization were conducted using a suite of techniques including IR spectroscopy, CNHSO elemental analysis, scanning electron microscopy and energy dispersive X-ray spectroscopy (SEM-EDS), and mass spectroscopy (MS). Density functional theory (DFT) calculations were employed to determine the molecular properties. Antioxidant activity was measured using the DPPH radical scavenging assay and the β-carotene bleaching test. Antimicrobial efficacy was assessed against four bacterial strains and three fungal strains. The molecular docking approach was employed to predict the probable binding patterns and affinities of arborescin with specific target biomolecules. Employing an array of analytical techniques, examination of the isolated crystal from *A. absinthium*. led to its comprehensive structural elucidation. IR spectroscopy revealed the presence of distinctive functional groups, including a carbonyl group within the γ-lactone and an epoxy group. CNHSO elemental analysis verified that the crystal contained only carbon, hydrogen, and oxygen, a finding corroborated by SEM-EDS analysis, consistent with the molecular structure of arborescin. Additionally, mass spectrometry confirmed the identity of the compound as arborescin, with a molecular ion with a mass *m/z* = 248. Quantum-Chemical Descriptors revealed that arborescin is resistant to elementary decomposition under standard conditions. Although arborescin demonstrates a relatively low antioxidant capacity, with an IC₅₀ of 5.04 ± 0.12 mg/mL in the DPPH assay, its antioxidant activity in the β-carotene bleaching test was

found to be 3.64%. Remarkably, arborescin effectively inhibits the growth of *Staphylococcus aureus* and *Listeria innocua* at low concentrations (MIC = 166 µg/mL). Additionally, it exhibits significant antifungal activity against *Candida glabrata*, with a minimum inhibitory concentration (MIC) and minimum fungicidal concentration (MFC) of 83 µg/mL and 166 µg/mL, respectively. In this study, arborescin exhibited a robust docking score of −8.1 kcal/mol, indicating a higher affinity compared to ciprofloxacin. This suggests that arborescin has significant potential as a potent antibacterial agent.

Keywords: arborescin; crystal structure; recrystallization; *Artemisia absinthium*; antimicrobial; antioxidant; docking

1. Introduction

Plants are an invaluable source of bioactive molecules, containing a variety of compounds with beneficial properties for health. These natural substances offer valuable therapeutic potential, making plants an essential resource in medical research and pharmacology [1]. As per the World Health Organization (WHO), a significant portion, approximately 80%, of the global populace relies on plants and herbs for medicinal purposes [2]. Moreover, plants offer a distinct advantage in the realm of drug discovery, attributed to their extensive historical utilization by humans. This extended usage suggests a potential for decreased toxicity in plant-derived medications, alongside an abundance of bioactive compounds [3]. Also, extracts or compounds from plants offer an alternative source of antimicrobials and antioxidants that is natural, more reliable, inexpensive, and time-tested compared to other antibiotics; also, they rarely have severe side effects [4]. Investigating the antioxidant, antibacterial, and antifungal properties of molecules isolated from plants offers promising potential for the discovery of new drugs. By isolating molecules, we can obtain a large number of molecules that can be used as active components in several fields, including agri-food, biotechnology, cosmetics, and pharmacology. *A. absinthium* holds significance as a perennial shrubby plant extensively employed in addressing various health conditions.

A. absinthium L., belonging to the Asteraceae family, is a perennial plant with yellow flowers that widely grows in sunny and dry regions of Europe, Siberia, South America, North America, and North Africa [5]. *A. absinthium* goes by several vernacular names. In English, it is recognized as absinthe, green ginger, wormwood, and absinthium. The French refer to it as Vermouth, and in Latin it is identified as Genepi. The Greek name is Apsinthion, and in Chinese it is known as Yang ai and Kuai [6]. In Hindi, it is known as Mastiyarah, Majtari, Karmala, or Majri. The Japanese term is nigayomogi, while in German it is recognized as Absinth or Wermut. In Arabic, it goes by names Afsanteen or Damseeh [7].

The plant's phytochemical examination has indicated the existence of chemical constituents, including polyphenolic compounds [8] and flavonoids [9] as well as fatty acids [10]. Also, the analysis suggests that the plant predominantly contains terpenoids, coumarins, caffeoylquinic acids, sterols, acetylenes, tannins, carotenoid glucosides, and sesquiterpene lactones or bitter principles [11–14]. Sesquiterpene lactones or bitter principles, characteristic of the Asteraceae family, exhibit properties such as antitumor, cytotoxic, antifungal, and antibacterial activities [14]. The stimulant effects of *A. absinthium* rely on the existence of bitter compounds like artabsine and absinthine, both of which are sesquiterpene lactones found in the plant's extracts [15]. Sesquiterpene lactones are a stable, bitter, and colorless subfamily of terpenoids, which are a class of lipophilic plant secondary metabolites, and they are almost exclusively derived from the Asteraceae family (Compositae) [16]. With over 11,000 sesquiterpenes recorded in the Dictionary of Natural Products, Sesquiterpene lactones make up a significant and biogenetically homogeneous group of natural compounds. Close to 5000 of these sesquiterpenes contain at least one lactone group; given their broad spectrum of biological activities, they act as an effective defense mechanism

for the organisms that synthesize them [17]. It has been demonstrated that this category of molecules is correlated with activities such as inhibiting tumor growth, inducing cell death, phytotoxic activity, and antimicrobial activity [18]. The diverse range of activities exhibited by sesquiterpene lactones implies that these natural compounds have evolutionary importance in plants, serving as deterrents against herbivores and exhibiting antibacterial and antifungal properties, as well as acting as allelopathic agents [14].

Absinthin, a dimeric sesquiterpene lactone, has been extracted from the plant *A. absinthium* using HPLC-solid phase extraction [19]. Two diastereometric homoditerpeneperoxides have been isolated from *A. absinthium* and the combination of these compounds demonstrated in vivo antimalarial activity, exhibiting an IC₅₀ of 1 µg/mL [20]. Another study identified sofalcone glycosides in the methanolic extract of the plant's aerial parts, characterized as artemisia isoflavonyl glucosyl diester and artemisia bis-isoflavonyl dirhamnoside [21]. Artemetin is a flavonoid isolated from leaves of *A. absinthium* [22]; it demonstrated hepatoprotective effects [23] as well as antimalaria activity [24]. Moreover, it exhibited anti-inflammatory and antioxidant actions [25] along with anticancer properties [26]. Being an unstable compound, it easily transforms into anabsinthin, and this molecule has exhibited anti-inflammatory activity in human bronchoepithelial cells [27]. Anabsin diguaianolide was isolated from *A. absinthium* L. [28]. Arborescin was isolated from *Artemisia gorgonum*, exhibiting a significantly lower IC₅₀ than the antitumoral drug etoposide, demonstrates notable cytotoxic activity in vitro, especially against tumoral cells, and is less toxic to nontumoral cells, suggesting its potential as a target for further studies to unravel the underlying mechanisms of its cytotoxic effects [29]. It was also isolated from flower baskets and leaves of *Artemisia austriaca* Jacq [30]. Crystalline arborescin was obtained from *Artemisia adamsii* [31].

The bibliography gives a very limited number of works and almost no interest has been devoted to thermal characteristics and biological activities. For this, in this study, our focus is on structural identification, employing a combination of techniques, such as elemental analysis, infrared and mass spectroscopy, and scanning electron microscopy. A theoretical investigation was carried out using density function theory to ascertain the parameters associated with this molecule. Exploring its potential applications in pharmacology, we proceeded to assess the molecule's activity as an antioxidant, antibacterial, and antifungal agent, and the obtained results were correlated with docking analyses.

The current challenges in treating infections caused by bacteria or fungi remain crucial, as it is often difficult to develop highly effective drugs with minimal adverse effects. Therefore, the discovery of medications derived from nature, particularly plant secondary metabolites, remains an attractive alternative for researchers and scientists. The molecule arborescin is under-studied, and its properties are poorly understood. Thus, our objective is twofold: first, to valorize this molecule isolated from a widely available plant; and second, to search for a new antimicrobial agent capable of competing in terms of cost and effectiveness with the antimicrobials already known.

2. Materials and Methods

2.1. Plant Material

The *A. absinthium* L. used in this study was first gathered in March 2021 from Zkara, a rural community in Mestferki, Morocco. This location is situated in the Oujda Angad prefecture, in the Oriental region of Morocco (Figure 1). The fresh leaves of the plant were harvested and dried in a dark, dry place at room temperature until all moisture was removed. They were then stored in a cool environment (4 °C) for later use. Just before use, the dried plant was reduced to a powder.

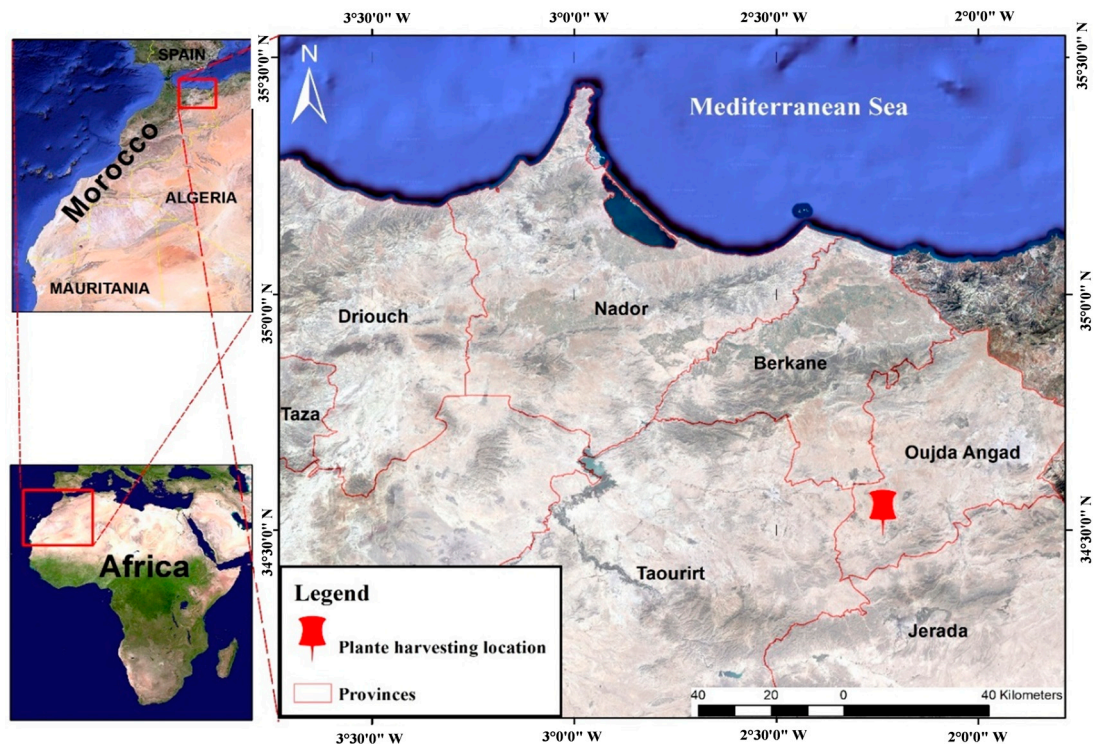


Figure 1. *A. absinthium* L. plant harvesting from the city of Oujda Angad in Morocco's southwest Oriental region.

2.2. Isolation Processus

The extraction of 50 g of *A. absinthium* powder involved using a 200 mL water/acetone mixture (3/7) and heating it at reflux for 2 h at a temperature of 65–70 °C. The resulting extract underwent concentration via vacuum evaporation until approximately one-third of the solvent was eliminated, after which it was extracted with 50 mL of hexane. The hexane fraction was retrieved and subjected to slow evaporation of the solvent in a dry location at a temperature between 10 and 15 °C. Transparent crystals began to form and grow during this process, and they were collected via vacuum filtration. A basic recrystallization procedure was then performed to obtain purified crystals. Initially, the impure crystals were dissolved in minimum of acetone, and then cold methanol was added. This process was repeated until a very pure crystal was obtained, confirmed by a single spot on thin-layer chromatography. The isolated crystals, weighing 11 mg, were stored in glass vials at a temperature of 4 °C.

2.3. High-Performance Liquid Chromatography

The purity analysis of the crystalline phase was conducted utilizing a liquid chromatography separation module (Waters e2695) in conjunction with a diode array detector (Waters 2998 PDA) from Waters Corporation company, united states. This detector records the ultraviolet and visible absorption spectra of the samples, providing qualitative information. The detector is integrated into the Empower data processing software. Analyses followed the protocol described by Hbika et al. [32]. Chromatograms were recorded between 254 and 300 nm using a C18 column (4.6 × 250 mm, 5 μm). The mobile phase, in gradient mode, consisted of ultrapure water/acetic acid (0.5%) (solvent A) and methanol (solvent B) with the following proportions: 0 min, 80% A and 20% B; 20 min, 0% A and 100% B; 25 min, 0% A and 100% B. The flow rate was 1 mL/min, and the injection volume was 20 μL.

Peaks were identified by comparing retention times and UV spectra with those of standards. The standard polyphenolic compounds used included gallic acid, vanillic acid, catechin, caffeic acid, salicylic acid, p-hydroxybenzoic acid, rutin, quercetin, syringic acid,

vanillin, naringenin, p-coumaric acid, artemetin, ascorbic acid, ferulic acid, malic acid, and kaempferol, which have been previously found in *A. absinthium*.

2.4. Elemental Analysis

The elemental analysis conducted on the CNHSO involved determining the relative proportions of carbon (C), sulfur (S), hydrogen (H), nitrogen (N), and oxygen (O) in the compound. This was achieved using the EuroEA 3000, which is a specialized instrument designed to analyze the elemental composition of organic compounds. The sample was carefully prepared and then subjected to high-temperature combustion, which converted the organic material into a gas that could be analyzed using the instrument. Instantaneous and complete oxidation of the sample to be analyzed is achieved by combustion with oxygen at a temperature of 1060 °C, with the furnace temperature set to 100 °C. The combustion products are then carried by the gas carrier to a column where separation occurs. The carrier pressure is 110 KPa. A thermal conductivity sensor provides the signal for each element, which is then translated into a percentage content. The operation time is 320 s and the sampling time is 5 s.

2.5. Fourier Transform Infrared Spectroscopy FT-IR

Fourier-transform infrared spectroscopy (FT-IR) analysis in the solid phase is carried out using an FTIR-4700 JASCO instrument, with recordings conducted within the 4000–400 cm^{-1} region. An interferogram is then recorded, composed of the detector signal as a function of time, and the resulting absorption spectrum is obtained by Fourier transformation of the interferogram [33].

2.6. Mass Spectroscopy

The technique of mass spectrometry (MS) is a critical physicochemical analytical tool for qualitative chemical analysis. To measure the exact masses of the atoms in the samples, a direct injection was performed using a Shimadzu GCMS-QP2010 instrument in electron impact mode.

This methodology entails the separation of charged molecules (ions) in the gas phase according to their mass-to-charge ratio (m/z). The function of a mass analyzer is to measure the mass-to-charge ratios (m/z) of ions. Its operating principles rely on the interaction of charged particles with electric or magnetic fields [34]. The mass spectrometer is comprised of an ionization chamber, an analyzer for separating the ions, and an ion detector. The resulting data allowed for the identification and quantification of the individual atoms present in the samples.

2.7. MEB/EDX

For the examination of both morphology and atomic composition, scanning electron microscopy (SEM-EDX) was employed, using a JEOL JSM-IT500HR model instrument. The crystal was positioned on a carbon strip affixed to a sample holder and subjected to observation under an operating voltage of 10 kV. This method facilitated a thorough investigation of the surface structure of the crystal and the elements comprising it. The combination of Energy-Dispersive X-ray Spectroscopy (EDX) and the Scanning Electron Microscope (SEM) enables high-resolution imaging and elemental analysis of samples.

2.8. Density Function Theory Study

The entire optimization process for the geometry of the isolated molecule was conducted utilizing density functional theory (DFT), employing the B3LYP hybrid functional [32]. Calculations were executed at the DFT/B3LYP level of theory using the 6-311 G (d,p) basis set integrated into Gaussian 09 W software, renowned for its sophisticated features in modeling electronic structures. These computations facilitated the determination of parameters characterizing the molecule's overall reactivity, such as total energy (ET), highest occupied molecular orbital energy (EHOMO), lowest unoccupied molecular orbital

energy (ELUMO), energy gap (ΔE_{gap}), dipole moment (μ), electron affinity (A_f), ionization potential (I), electronegativity (χ), global softness (σ), global hardness (η), electrophilicity (ω), and chemical potential (μ) [22].

2.9. Antioxidant Activity

2.9.1. Scavenging 2,2-Diphenyl-1-picrylhydrazyl Radical Test

The antioxidant potential of arborescin was evaluated through the DPPH (1,1-diphenyl-2-picrylhydrazyl) radical decolorization assay [35,36], a well-established method for assessing the antioxidative properties of natural substances by measuring their capability to neutralize free radicals. In this assay, varying concentrations of arborescin solution (ranging from 0.0625 to 2 mg/mL) were combined with freshly prepared methanolic DPPH solution (0.1 mM) in a ratio of 500 μ L to 3 mL, respectively. To establish a negative control, 500 μ L of the solvent utilized for extract solubilization was mixed with a 3 mL solution of DPPH prepared in methanol. Subsequently, the absorbance of the decolorized DPPH solution was determined against a blank solution at a wavelength of 517 nm following a 20 min incubation period at room temperature and in darkness, utilizing a UV/visible spectrophotometer. Ascorbic acid served as the positive control, and its absorbance was measured under identical conditions and procedures as those employed for the sample. Each concentration was subjected to triplicate measurements. The scavenging activity was quantified using the formula provided below:

$$\text{trapping activity}(\%) = \frac{A_0 - A_1}{A_0} \times 100 \quad (1)$$

where A_0 represents the absorbance of the control reaction, and A_1 represents the absorbance of the test sample.

2.9.2. β -Carotene Bleaching Test

The carotene bleaching test was used to evaluate the antioxidant capacity of arborescin, following the procedure described by Kartal et al. [37,38]. The β -carotene/linoleic acid emulsion was prepared by dissolving 2 mg of β -carotene in 1 mL of chloroform, along with 25 μ L of linoleic acid and 200 mg of Tween 80. The chloroform was then evaporated using a rotary evaporator. Subsequently, 100 mL of distilled water saturated with 30% H_2O_2 was added to the dried mixture, and the resulting emulsion was thoroughly stirred to ensure uniformity. Following this, 175 μ L of the test molecule solution or a solution of butylated hydroxyanisole (BHA) at a concentration of 2 mg/mL was added to 1.25 mL of the emulsion. The decolorization kinetics of the negative control emulsion, arborescin, and the BHA were monitored at 490 nm over 120 min at regular intervals. The relative antioxidant activity (RAA) of the molecule was determined using the formula below:

$$\text{RAA}(\%) = \frac{A_{120} - C_{120}}{C_0 - C_{120}} \times 100 \quad (2)$$

where A_{120} represents the absorbance values of the solution containing arborescin after 120 min of incubation, and C_0 and C_{120} represent the absorbance values of the control before and after 120 min of incubation, respectively.

2.10. Antimicrobial Activity

1. Bacterial strains

In this investigation, we employed four bacterial strains: *Escherichia coli* (ATCC 10536), *Staphylococcus aureus* (ATCC 6538), *Listeria innocua* (ATCC 33090), and *Pseudomonas aeruginosa* (ATCC 15442), serving as representative microorganisms to assess the antibacterial effectiveness of the four synthesized molecules. These strains were sourced from the Laboratory of Bioresources, Biotechnology, Ethnopharmacology, and Health, situated within the Faculty of Sciences at Oujda, Morocco [39].

2. Fungal strains

For this investigation, three distinct fungal strains, *Aspergillus niger*, *Candida glabrata*, and *Penicillium digitatum*, were chosen to evaluate the antifungal capabilities of the four molecules under scrutiny. These fungal strains were sourced from the Laboratory of Bioresources, Biotechnology, Ethnopharmacology, and Health, housed within the Faculty of Science at Oujda, Morocco.

3. Determination of MIC, MBC, and MFC

Determining the minimum inhibitory concentration (MIC) is a critical step in assessing the efficacy of antimicrobial agents. The determination of the minimum inhibitory concentration (MIC) for the four molecules under investigation utilized the resazurin microtitration assay. This assay was conducted in 96-well microplates, with each well containing concentrations ranging from 15 mg/mL to 0.05 mg/mL of the test compounds. A standardized inoculum of the respective microbial strain was introduced into each well, followed by incubation at the appropriate temperature: 37 °C for bacterial strains and 25 °C for fungal strains, both for a duration of 18 h. Following incubation, resazurin was introduced into the microplates, and a subsequent 2 h incubation period ensued until a color change from blue to pink was evident [40].

MBC and MFC were determined by inoculating a 3 µL sample taken from negative wells onto agar media plates, which were then incubated at the appropriate temperature for each type of microbial strain for 24 h. The lowest concentration of samples that did not result in microbial growth was used to establish MBC and MFC [39].

2.11. Molecular Docking Protocol

The utilization of the molecular docking methodology facilitated the anticipation of plausible binding configurations and affinities between isolated plant metabolites and specific target biomolecules [41]. Employing a computational docking strategy, we projected the potential antioxidant and antibacterial properties of arborescin, adhering to the methodologies outlined in prior studies [41,42]. In accordance with established literature, we carefully selected distinct proteins for interaction: xanthine oxidoreductase (PDB ID: 3AX7) for antioxidant evaluation [43], and dihydrofolate reductase (DHFR) enzyme (PDB ID: 4M6J) for assessing antibacterial effects [44]. Acquisition of the three-dimensional crystal structures of these designated proteins was accomplished from the RCSB Protein Data Bank (source: <https://www.rcsb.org>; accessed on 1 February 2024) in PDB format.

1. Subsequent to this step, we employed the PyMoL 2.3 tool to preprocess all macromolecules, eliminating water molecules and extraneous protein residues. In order to guarantee structural integrity, nonpolar hydrogen atoms were integrated into the refined proteins. Sequentially, the Swiss PDB viewer, renowned for its energy minimization capabilities [45], was employed to minimize their energy states to the lowest possible level. After these purification and optimization processes, the macromolecules were archived in PDB format and primed for subsequent analysis.
2. Throughout the computational interaction process, we implemented a semi-flexible modeling approach utilizing the extensively employed PyRx AutoDock Vina molecular docking software. Within PyRx, the target proteins were prepared and designated as macromolecules [46]. The 3D conformers of all ligands, initially in SDF format, were introduced into PyRx and subjected to energetic optimization. Subsequently, they were converted to pdbqt format using the Open Babel tool within the PyRx AutoDock Vina software, with a selection of the most optimal hit [47]. The results of the docking analysis were projected, and the outcomes, in conjunction with the docked macromolecules and ligands, were exported as output files in pdbqt format. These ligand and macromolecule files were merged and preserved in PDB format for further scrutiny using PyMol software. Ultimately, 2D visualizations were generated utilizing Discovery Studio Visualizer (version 4.6).

3. Results and Discussion

3.1. High-Performance Liquid Chromatography Analysis

The process of isolating a molecule in the liquid phase often involves the coexistence of various other molecules, even at low concentrations. In order to purify the solid phase, we adopted a sequential process of dissolution and recrystallization to minimize the presence of parasitic molecules, and the verification was conducted using thin layer chromatography until a spot was obtained. High-performance liquid chromatography (HPLC) characterization of the resulting crystal did not show any peaks; this suggests that this molecule does not fall within the range of compounds that absorb wavelengths between 254 and 300 nm. The diode array detector used is specifically designed for the identification of elements with wavelengths generally ranging from 190 to 400 nm (ultraviolet).

The lack of results for chromatographic analysis, attributed to the absence of UV absorbance, may be explained by the presence of a molecule lacking a distinct chromophore and featuring a peroxy bridge. Indeed, although high-performance liquid chromatography with ultraviolet detection is widely available, it has not been used for the analysis of certain sesquiterpene lactones, such as artemisinin, due to the reported lack of UV absorption for this lactone [48]. Determining artesunate is also challenging, similar to artemisinin, due to the absence of a distinct chromophore and the presence of a peroxy bridge that absorbs at higher wavelengths [49–51]. Additionally, absorbance responses increase with the presence of double bonds. The detection limit of HPLC-DAD is also not low enough, rendering this method incapable of detecting dihydroartemisinin, a sesquiterpene lactone [48].

3.2. Infrared Spectroscopy

The spectral range spanning from 1000 to 4000 cm^{-1} , often referred to as the functional groups region, is paramount in furnishing the bulk of information utilized for the interpretation of an IR spectrum. Conversely, the segment spanning between 400 and 1000 cm^{-1} , recognized as the fingerprint region, encompasses a multitude of peaks and tends to exhibit greater complexity, rendering the assignment of individual peaks more challenging.

The IR spectrum of the compound CR1 presented in Figure 2 contains characteristic absorption bands in the range of 3058 and 2910 cm^{-1} , which are indicative of C-H bonds. There is a more intense and sharper band at 1770 cm^{-1} characteristic of the carbonyl in the γ -lactone, a band at 1430 cm^{-1} which corresponds to deformation vibrations in the plane of C-H bonds, and a band at 1128 cm^{-1} attributed to the epoxy group C-O-C.

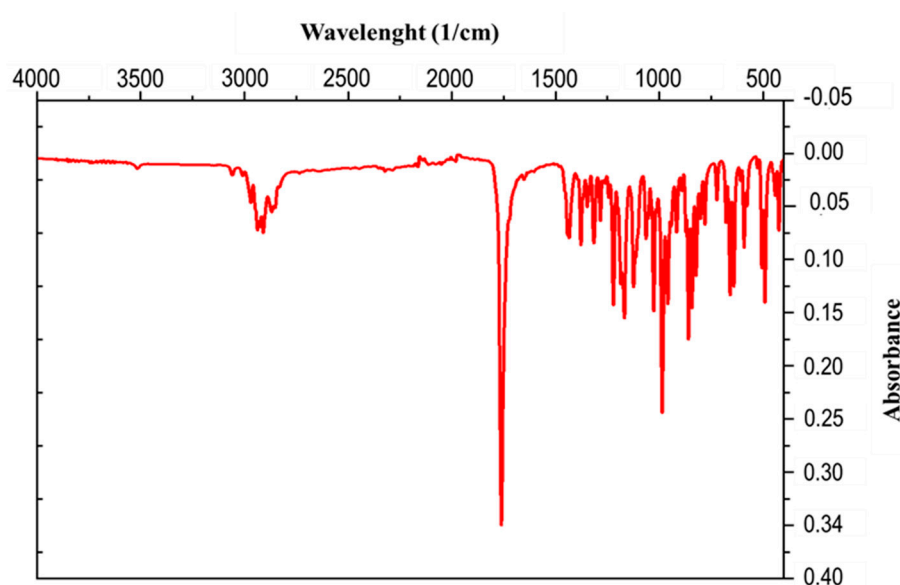


Figure 2. IR spectrum of isolated crystal.

3.3. Scanning Electron Microscopy and Energy-Dispersive Spectroscopy

Scanning electron microscope observations of the solid crystal have revealed a crystalline morphology characterized by square layers that have sedimented onto each other. The clearly defined lines observed vividly illustrate the sedimentation process, where these square layers overlap in an organized manner (Figure 3).

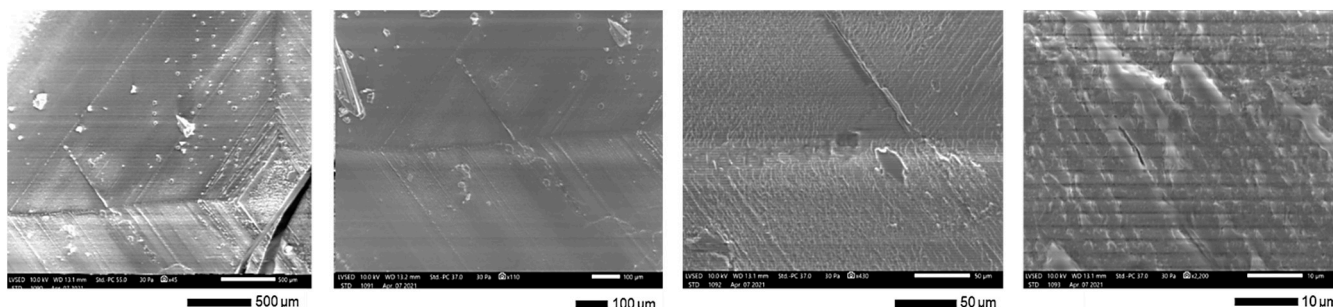


Figure 3. Crystal morphology.

The results of the energy dispersive X-ray spectroscopy (EDS) analysis conducted on the crystal’s chemical composition distinctly indicate that the predominant atoms of the compound are carbon and oxygen, as depicted in Table 1. The obtained molar ratio of C/O is 4.93, highlighting the relative proportion of these elements in the material’s composition.

Table 1. Atomic chemical composition of the isolated crystal.

Element	Mass %	Atom %
C	78.7 ± 0.46	83.2 ± 0.49
O	21.2 ± 0.71	16.8 ± 0.56
Total	100.00	100.00

3.4. Mass Spectrometer

The mass spectrometer (MS) of the compound obtained in electron impact mode reveals a molecular ion with a mass $m/z = 248$ (Figure 4), suggesting a molar mass of 248 g/mol. This mass corresponds to that of arborescin with the formula $C_{15}H_{20}O_3$ (Figure 5). The various possible fragments are shown in Figure 6. The MS spectrum provides the following ions:

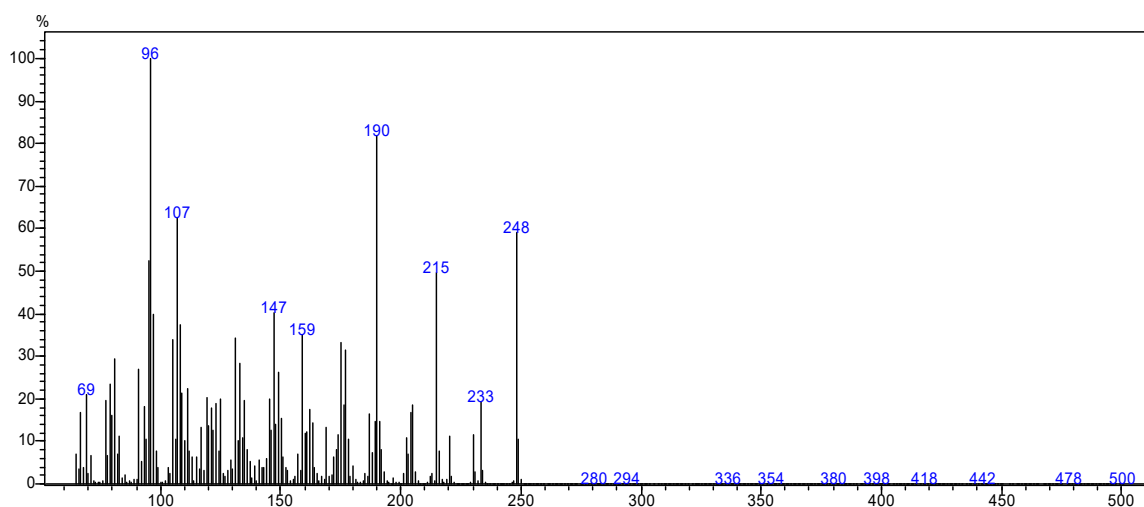


Figure 4. Mass spectrum of the crystal.

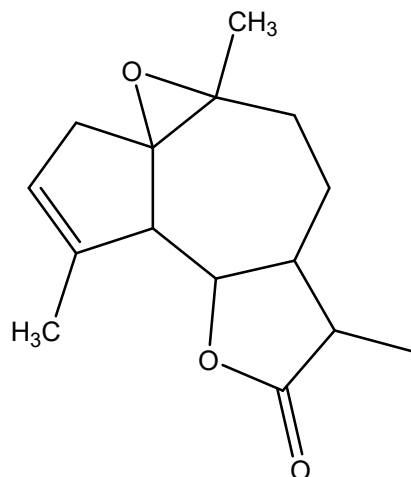


Figure 5. Probable chemical structure of the isolated crystal.

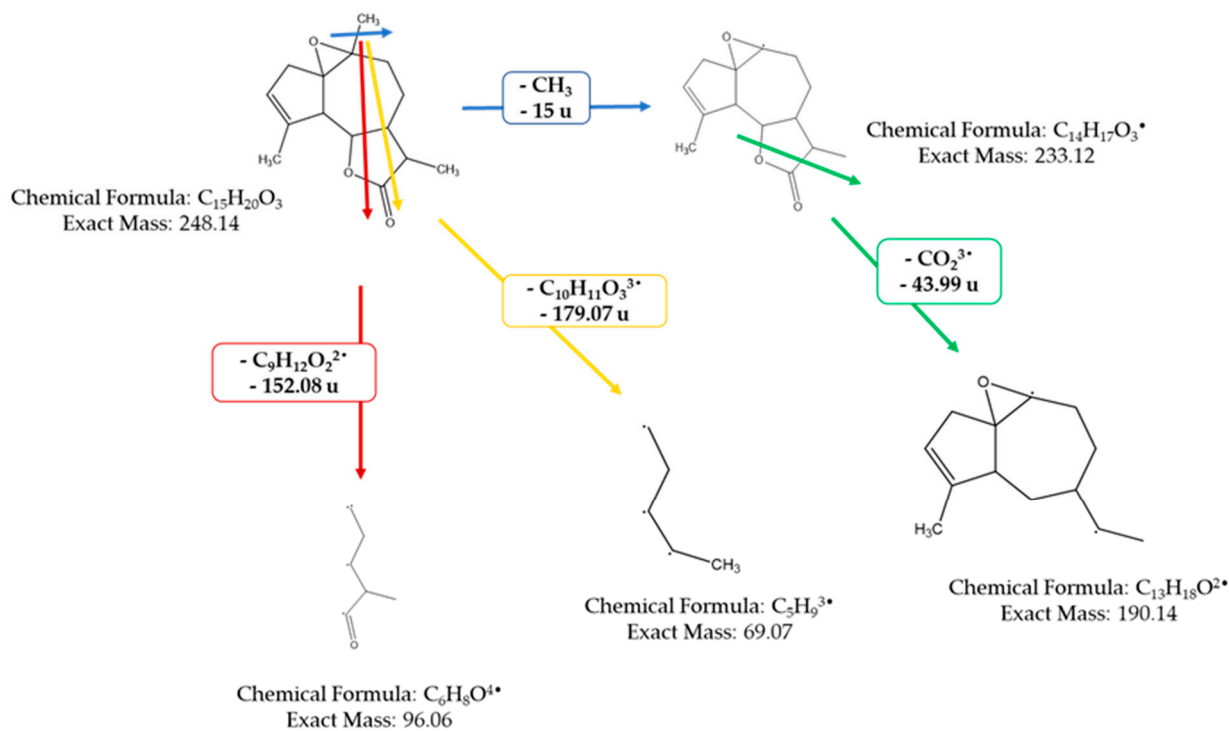


Figure 6. Various possible fragments of the MS spectrum.

An ion detected at m/z 233, representing a loss of 15 u from m/z 248, implies the potential loss of CH_3^{\bullet} .

An ion observed at m/z 96, which corresponds to a loss of 152 u from m/z 248, indicates the potential loss of a fragment with the molecular formula of $C_9H_{12}O_2^{2\bullet}$.

An ion at m/z 69 (loss of 179.07 u from m/z 248) suggesting the loss of $C_{10}H_{11}O_3^{3\bullet}$.

An ion at m/z 190, indicating a loss of 44 u from m/z 233, suggests the potential loss of $CHO_2^{3\bullet}$.

An ion at m/z 147 (loss of 43 u from m/z 190) suggesting the loss of $C_2H_3O^{3\bullet}$.

An ion at m/z 107, signifying a loss of 40 u from m/z 147, suggests the loss of $C_3H_4^{2\bullet}$.

An ion at m/z 215, indicative of a loss of 44 u from m/z 233, suggests the loss of $CHO_2^{3\bullet}$. These findings offer invaluable insights into the molecular structure and fragmentation patterns of the compound, enabling a comprehensive characterization of its molecular composition.

3.5. Elemental Analysis CNHSO

The elemental analysis of CNHSO, conducted on the solid phase, yielded weight ratios of C/O close to those of the empirical formula of arborescin, as shown in Table 2. The results demonstrate that the isolated molecule consisted solely of carbon, oxygen, and hydrogen atoms. The experimental and theoretical ratios obtained were 9.29 and 9.00, respectively. This slight difference could be attributed either to instrument error or the potential presence of impurities in the isolated molecule.

Table 2. CNHSO elemental analysis results.

Mass	Arborescin C ₁₅ H ₂₀ O ₃	
	Experimental	By Formula
C%	73.1	72.6
O%	7.86	8.06
H%	19.0	19.3
N%	0.00	0.00
S%	0.00	0.00
C/O	9.29	9.00

3.6. Quantum Chemistry Calculations

In Figure 7, the refined arrangement of arborescin is illustrated alongside the three-dimensional depictions of its frontier orbitals, namely the Highest Occupied Molecular Orbital (HOMO) and the Lowest Unoccupied Molecular Orbital (LUMO), as observed in its fundamental state. Within these depictions, the HOMO and LUMO orbitals exhibit discernible phases denoted by red and green, respectively, highlighting positive and negative charge distributions. A thorough examination of the three-dimensional representations of arborescin's frontier orbitals reveals a notable concentration of electron charges predominantly localized on the pentane cycle and the CH₃ group attached to it.

Table 3 presents the computed energies and various parameters utilizing the B3LYP 6-311G (d,p) method. The energy associated with the Highest Occupied Molecular Orbital (HOMO) directly correlates with the ionization potential, whereas the energy corresponding to the Lowest Unoccupied Molecular Orbital (LUMO) is directly associated with the electron affinity. These computations offer valuable insights into the electronic and reactive characteristics of arborescin, contributing to a comprehensive comprehension of its molecular chemistry. Analysis of the results indicates that a significant energy gap (ΔE_{gap}) signifies heightened molecular stability and reduced aromaticity, whereas a minimal disparity between HOMO and LUMO suggests the system's flexibility and high polarizability [52,53]. Arborescin exhibits negative values for both EHOMO and ELUMO energy levels, indicating its stability. With a low energy gap (ΔE_{gap}) of 6.73 eV, the molecule demonstrates high chemical activity, categorizing it as "soft". Such molecules possess a higher reactivity compared to their "hard" counterparts. Additionally, the global hardness obtained is low, at 3.36 eV. The dipole moment offers insights into the polarity of the entire molecule [54].

Electrophilicity pertains to an electrophile's capacity to gain an extra electron charge and its resilience to exchanging electron charges with the environment [55]. The negative chemical potential (−3.41 eV) indicates the molecule's resistance to decomposition into elements. Accordingly, a substantial dipole moment of 5.47 D is evident, indicating pronounced molecular polarity, likely augmenting its high chemical reactivity.

Table 3. Quantum parameters of global reactivity descriptors calculated.

Descriptors of Global Reactivity	Arborescin
Total global energy (ET)	−809.5 (u a)
Lowest unoccupied molecular orbital (E_{LUMO})	−0.04 (eV)
Highest occupied molecular orbital (E_{HOMO})	−6.77 (eV)
Energy gap (ΔE_{gap})	6.73 (eV)
Absolute electronegativity (χ)	3.41 (eV)
Overall hardness (η)	3.36 (eV)
Electron affinity (A_f)	0.04 (eV)
Ionization (I)	6.77 (eV)
Electrophilicity (ω)	1.72 (eV)
Overall softness (σ)	0.30 (eV)
Dipole moment (η)	5.47 (D)
Chemical potential (μ)	−3.41 (eV)

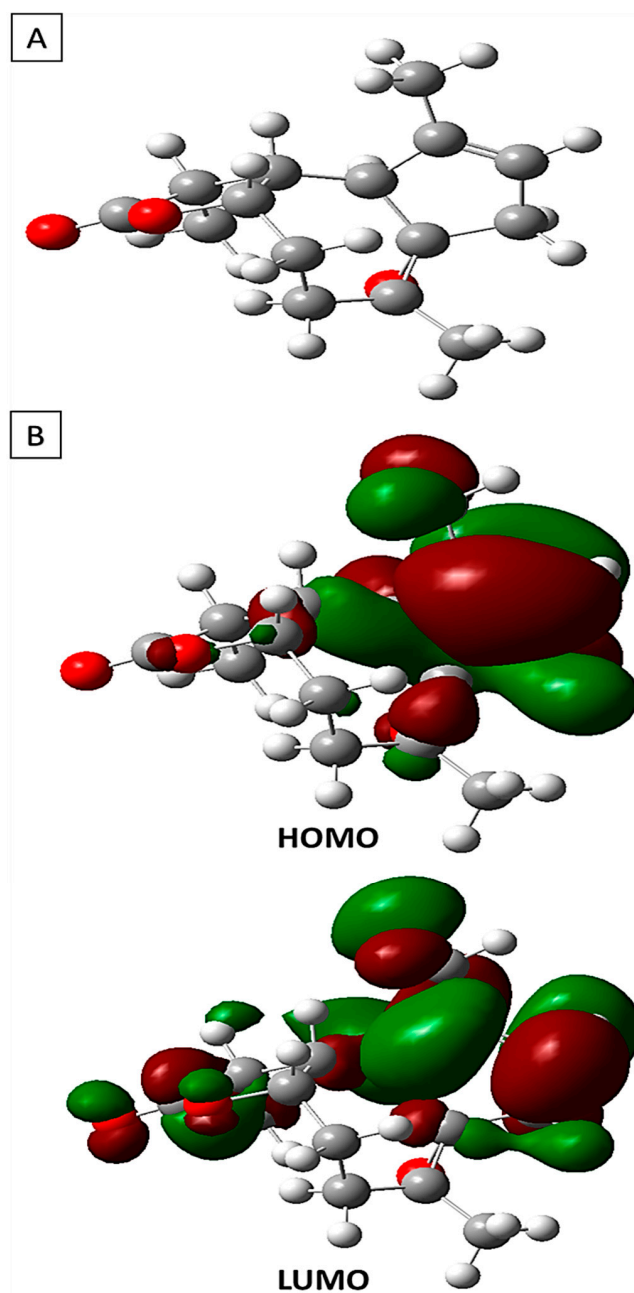


Figure 7. (A) The optimized configuration of arborescin in its neutral state alongside (B) the Highest Occupied and the Lowest Unoccupied Molecular Orbitals determined by DFT.

3.7. Antioxidant Activity

3.7.1. DPPH Radical Trapping Test

Figure 8 illustrates the antioxidant powers of arborescin. Overall, the tested compound exhibited a low DPPH consumption, with inhibition percentages not exceeding 20% for a concentration of 2 mg/mL. The IC₅₀ test values are provided in Table 4. Arborescin demonstrates modest antioxidant activity, evidenced by an IC₅₀ value of 5.04 ± 0.12 , significantly distant from that of ascorbic acid, which gives an IC₅₀ value of 0.16 ± 0.003 mg/mL.

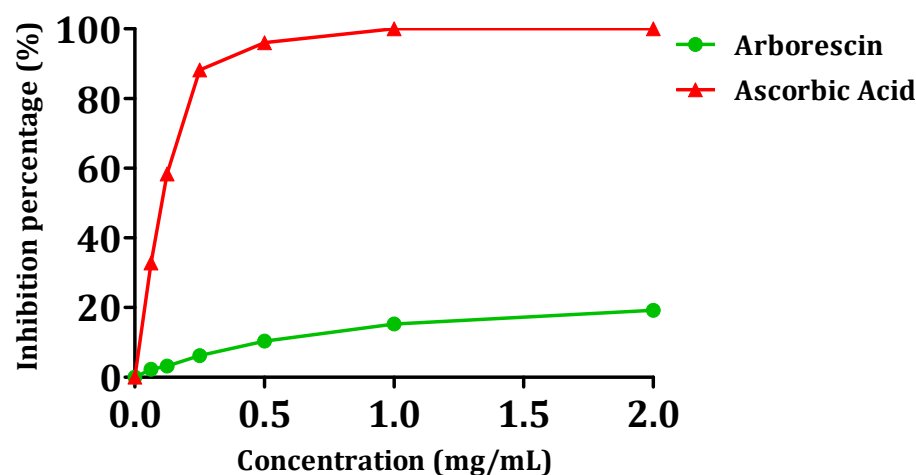


Figure 8. Scavenging activity of the DPPH radical in the presence of arborescin.

Table 4. IC₅₀ values obtained in the presence of arborescin for the DPPH and FRAP assays, along with the percentage Relative Antioxidant Activity (% RAA) for the β -carotene bleaching assay.

	DPPH (mg/mL)	β -Carotene (RAA %)
BHA	-	73.4
Ascorbic acid	0.16 ± 0.003	-
Arborescin	5.04 ± 0.12	3.64

Consistent with the pattern observed in most polyphenolic antioxidants, the configuration and total number of hydroxyl groups in the flavonoid structure significantly influence their antioxidant activity [56]. This observation may justify the moderate antioxidant capacity found for arborescin in this study.

3.7.2. Bleaching Kinetics of the β -Carotene Assay

The results of arborescin's ability to inhibit or delay lipid peroxidation are presented in Figure 9. The results suggest that this particular compound lacks significant inhibitory effects on the oxidation of linoleic acid when compared to the negative control. It is noteworthy that the inhibition of oxidation is very low for arborescin, with a percentage of 3.64%. The observed value remains notably lower compared to that of the reference compound BHA (Table 4). It can be observed that the absorbance of arborescin and the negative control decrease linearly over time, unlike that of BHA. Even molecules with a weak or moderate antioxidant effect can be beneficial. Molecules with low antioxidant activity can indeed have a synergistic effect when combined with other antioxidants. If, for example, both molecules have moderate antioxidant properties, they can work together to regenerate each other and enhance overall antioxidant protection. Low antioxidant activity can also offer gradual and continuous protection against oxidative damage, which is especially beneficial for the long-term prevention of chronic diseases like cardiovascular diseases and certain cancers.

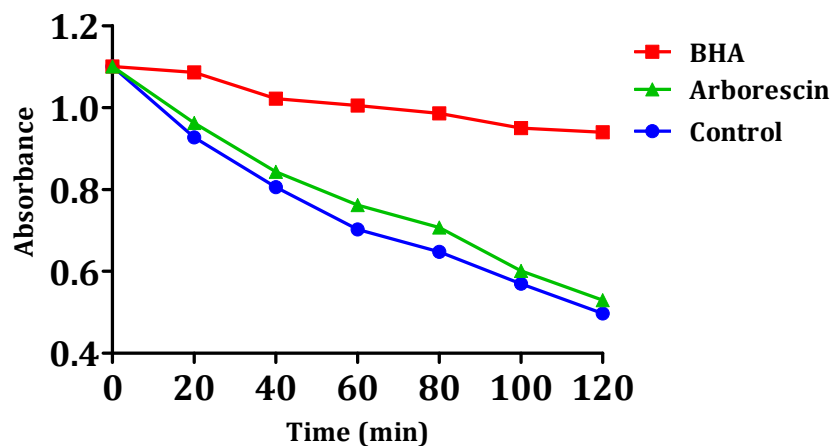


Figure 9. Kinetics of β -carotene bleaching in the presence of arborescin and BHA.

In the presence of the compound, the free radical of linoleic acid experiences an attack by β -carotene, resulting in rapid bleaching, which is attributed to the depletion of double bonds in linoleic acid [57]. This is in contrast to BHA, where absorbance decreases gradually, indicating the inhibition of linoleic acid oxidation.

3.8. Antibacterial Activity

Evaluation of the antibacterial activity of the arborescin molecule revealed notable results (Table 5), highlighting its effectiveness against different bacterial strains. Minimum inhibitory concentrations (MICs) varied according to the bacteria tested, with values of 83 $\mu\text{g/mL}$ for *E. coli*, 166 $\mu\text{g/mL}$ for *S. aureus* and *L. innocua*, and again 83 $\mu\text{g/mL}$ for *P. aeruginosa*. These data demonstrate the ability of arborescin to inhibit bacterial growth at relatively low concentrations. The minimum bactericidal concentration (MBC) reflects the lowest concentration at which the molecule completely eradicates bacteria. The MBC for *E. coli* is 333 $\mu\text{g/mL}$, while for *S. aureus* it is indicated as being greater than or equal to 666 $\mu\text{g/mL}$, demonstrating bactericidal activity at higher concentrations. For *L. innocua*, the MBC is 666 $\mu\text{g/mL}$, and for *P. aeruginosa*, it is 333 $\mu\text{g/mL}$.

Table 5. Antibacterial Efficacy Evaluation.

Bacterial Strains		<i>E. coli</i>	<i>S. aureus</i>	<i>L. innocua</i>	<i>P. aeruginosa</i>
Arborescin	MIC ($\mu\text{g/mL}$)	83	166	166	83
	MBC ($\mu\text{g/mL}$)	333	≥ 666	≥ 666	333

These results demonstrate the specific antibacterial activity of arborescin against different bacterial strains. It should be noted that this molecule is known for its diverse biological activities, such as its anticancer potential. Martins et al. [58] highlighted that arborescin, in particular, is the most promising compound, capable of reducing the viability of tumor cells. These results highlight the versatile potential of arborescin and encourage further investigation into its application, whether in a clinical or industrial context.

3.9. Antifungal Activity

Evaluation of the antifungal activity of the arborescin molecule produced notable results (Table 6), revealing its efficacy against various fungal strains. Minimum inhibitory concentrations (MICs) varied according to the strains tested, with values of 41 $\mu\text{g/mL}$ for *Aspergillus niger*, 83 $\mu\text{g/mL}$ for *Candida glabrata*, and again 41 $\mu\text{g/mL}$ for *Penicillium digitatum*. These data indicate that arborescin has the capacity to inhibit fungal growth at relatively low concentrations.

Table 6. Assessment of Antifungal Activity.

Molecule	Fungal Strains	<i>Aspergillus niger</i>	<i>Candida glabrata</i>	<i>Penicillium digitatum</i>
Arborescin	MIC ($\mu\text{g/mL}$)	41	83	41
	MBC ($\mu\text{g/mL}$)	166	41	166

The minimum fungicidal concentration (MFC) represents the lowest concentration at which the molecule completely eradicates fungi. The MFC for *Aspergillus niger* is greater than or equal to 166 $\mu\text{g/mL}$, for *Candida glabrata* it is 41 $\mu\text{g/mL}$, and for *Penicillium digitatum* it is 166 $\mu\text{g/mL}$.

These results highlight the specific antifungal activity of arborescin against different fungal strains. They also indicate that the molecule's efficacy varies according to the type of fungus under consideration. This inherent specificity has significant implications for the future development of arborescin as an antifungal agent. The results serve as a catalyst for further research to elucidate the precise mechanism by which arborescin combats fungi. This investigation aims to discern its potential applications in clinical or industrial contexts, with a particular focus on the treatment of fungal infections.

3.10. Molecular Docking Predictions Revealing Potential Mechanisms of Action for Arborescin

To investigate the impact of arborescin, a sesquiterpene lactone, on pharmacological functions, we employed diverse computer-based techniques to conduct molecular docking with relevant molecular receptors. The binding strength correlates inversely with the numerical value of binding affinity, typically measured in kcal/mol. The initial docking prediction revealed an expected binding affinity, marked by a root mean square deviation of zero [38].

In this study, we utilized a method to evaluate the binding affinities of arborescin. The compound was tested against two important proteins associated with the tested biological functions: Xanthine oxidoreductase (PDB ID: 3AX7) was examined for antioxidant activity [43], and Dihydrofolate reductase (DHFR, PDB ID: 4M6J) was examined for its antibacterial activity, as reported by [59]. The results of the molecular docking investigations are presented in Table 7.

Table 7. The computational simulations in CAEO yield the molecular free binding affinity of the identified compounds, measured in kcal/mol.

N°	Compounds	3AX7	4M6J
		(Antioxidant)	(Antibacterial)
Free Binding Energy (kcal/mol)			
-	Native Ligand	−8.0 (Oxypurinol)	−8.0 (Ciproflaxacin)
1	Arborescin	−8.0	−8.1

3.10.1. Interactions with Xanthine Oxidoreductase (PDB: 3AX7): Antioxidant Activity

Xanthine oxidoreductase (XOR) is an enzyme involved in purine metabolism, catalyzing the conversion of hypoxanthine to xanthine and subsequently to uric acid [60]. While this enzyme plays a crucial role in normal physiological processes, such as the breakdown of nucleotides, it also generates reactive oxygen species (ROS) as byproducts, particularly during the conversion of hypoxanthine to xanthine and xanthine to uric acid [61]. These ROS can lead to oxidative stress and contribute to various pathological conditions, including inflammation, cardiovascular diseases, and neurodegenerative disorders [62,63].

The significance of inhibiting XOR lies in its potential to reduce the production of ROS and subsequent oxidative damage [43]. By inhibiting XOR activity, either through direct inhibition or modulation of its expression, it is possible to decrease ROS production, thereby

mitigating oxidative stress and its associated detrimental effects [64]. This inhibition can be particularly relevant in the context of antioxidant activity, as it helps to balance the oxidative state within cells and tissues.

Our investigation unveiled that arborescin exhibited a noteworthy binding affinity of -8.0 kcal/mol, akin to the native inhibitor allopurinol, which also displayed a binding affinity of -8.0 kcal/mol (refer to Table 7). Remarkably, arborescin engaged in four hydrogen bonds with amino acid residues situated within the binding site pocket, specifically Leu580, Glu757, Arg793, and Ile1063. In contrast, allopurinol did not form any hydrogen bonds with the amino acid residues within the binding pocket (Figure 10).

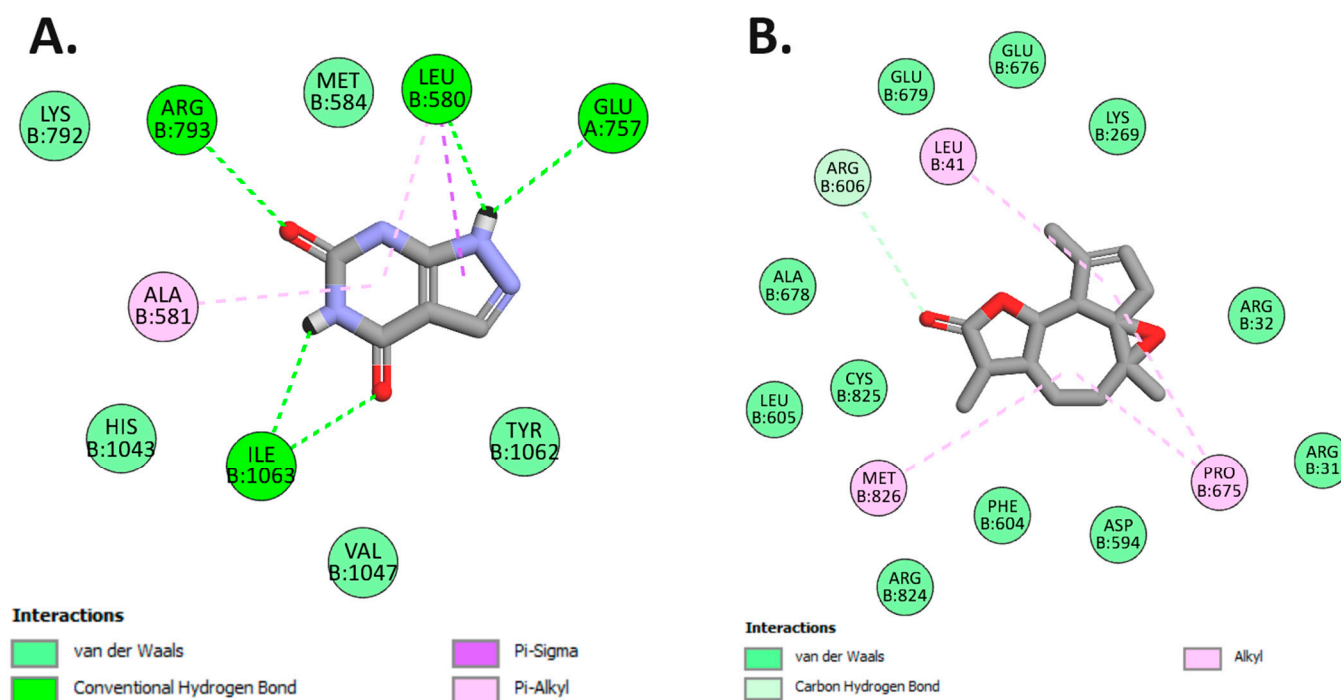


Figure 10. 2D Molecular docking interactions of arborescin (A) and allopurinol (B) with xanthine oxidoreductase (PDB: 3AX7).

3.10.2. Interactions with Dihydrofolate Reductase (PDB: 4M6J): Antibacterial Activity

Dihydrofolate reductase (DHFR) serves a vital function in the synthesis of tetrahydrofolate, a crucial precursor required for the biosynthesis of purines, pyrimidines, and specific amino acids [65]. Targeting DHFR inhibition has been a focal point in the development of antibacterial, antifungal, antituberculosis, and anticancer drugs due to its role in impeding cellular replication and growth [66,67].

The protein structure, identified by its PDB ID 4M6J, was retrieved from the RCSB Protein Data Bank and represents the crystallographic depiction of DHFR (Dihydrofolate Reductase) derived from *Staphylococcus aureus* [68]. This structural revelation presents a compelling opportunity for the advancement of antibacterial treatments, particularly considering the virulent nature of *S. aureus*, a pathogenic bacterium known to cause a spectrum of infections including skin and soft tissue disorders, bone infections, and others [68]. Focusing on DHFR emerges as a strategically pivotal pursuit as the inhibition of this enzyme interrupts the biosynthesis of tetrahydrofolate. This disruption ultimately leads to the depletion of crucial folate coenzymes necessary for the synthesis of nucleic acids, including DNA and RNA as well as certain amino acids [69]. As a result, DHFR emerges as a captivating focal point for the progression of antibacterial medications, demonstrating the potential to effectively hinder bacterial growth and proliferation [70].

In this investigation, arborescin demonstrated a robust docking score of -8.1 kcal/mol, surpassing that of ciprofloxacin, a broad-spectrum antibiotic belonging to the fluoro-

quinolones group. This finding suggests the potential of arborescin as a potent antibacterial agent, as highlighted in Table 7. While ciprofloxacin formed three hydrogen bonds with amino acid residues within the protein's binding pocket—Ser3, Val109, and His130—arborescin only engaged in a single hydrogen bond with Arg137 at the active site, as depicted in Figure 11.

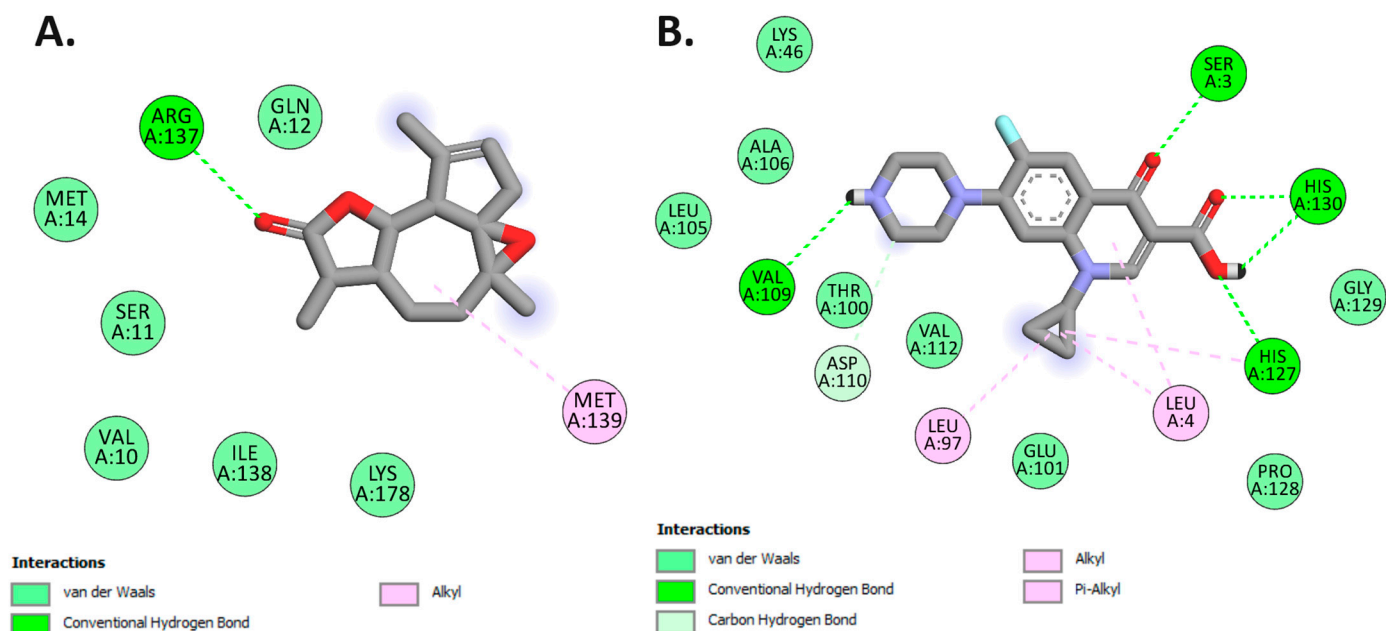


Figure 11. Two-dimensional molecular docking interactions of arborescin (A) and Ciprofloxacin (B) with dihydrofolate reductase (PDB: 4M6J).

The potential integration of arborescin, a sesquiterpenic lactone that has shown significant antimicrobial potential, could play a crucial role in the treatment and prevention of various pathogenic infections. Indeed, the compounds isolated from species of Asteraceae, belonging to the sesquiterpenic lactones family, have a wide range of biological effects; some of these compounds are already available on the market, such as artemisinin [71], which has shown anticancer [72] and antimalarial effects [73].

In some cases, sesquiterpene lactones are regarded as the primary active components of these medicinal plants [74]. Some of these compounds were found to have antitumor [75], anti-inflammatory, antimicrobial, antimalarial [76], neuroprotective [77], immunostimulant, and hepatoprotective properties [78]. Studies conducted with arglabin demonstrate its potential for the development of new anticancer and anti-inflammatory drugs [79]. Cynaropicrin, falling within the same category of compounds, has demonstrated antitumor, antitrypanosomal, and anti-inflammatory properties, alongside its antiviral efficacy against hepatitis C [80]. Costunolide has been proven to be a potent anticancer agent and anti-inflammatory, as well as exhibiting antimicrobial and antidiabetic properties [81,82].

In terms of the relationship between the structure and activity of these compounds, it seems that the α -methylene- γ -lactone nucleus plays a vital role in most of their documented biological effects [16,83].

Due to its functional groups, Artemetin holds promise for evaluation as a therapeutic agent with potential anti-inflammatory, antidiabetic, and anticancer properties, offering a diverse range of pharmaceutical potentials.

The main limiting factor in this perspective is the relatively low yield generated by the isolation process.

4. Conclusions

Bioactive molecules serve as a central focus in the exploration of aromatic and medicinal plants, owing to their notable biological activities. A lot of compounds possess intricate structures that confer upon them elevated levels of both chemical and biological reactivity. Our research specifically delves into the properties of “Arborescin”, a member of the sesquiterpenic lactone family extracted from *A. absinthium* L. The extraction process involved the use of hexane, after refluxing with a mixture of acetone and water. Mass spectroscopy, infrared spectroscopy, scanning electron microscope, X-ray energy dispersive spectroscopy, and CNHSO elemental analysis were conducted to elucidate the molecular structure; then, thermal analysis was performed for the arborescin molecule (C₂₀H₂₈O₈) and rigorously examined. Following structural identification and determination of the quantum parameters of the descriptors, the antifungal and antibacterial activity of arborescin was evaluated, and the results show that it possesses interesting antimicrobial activity against the strains used, which has been correlated to docking.

Author Contributions: Conceptualization, A.H. and E.G.; methodology, A.H., A.B., E.G. and M.I.Y.; software, M.A. and A.E.; validation, A.A., A.B. and E.G.; formal analysis, A.H. and E.G.; investigation, A.E. and M.T.; resources, A.A.; data curation, E.H.L.; writing—original draft preparation, A.H. and E.G.; writing—review and editing, A.H., E.G., A.E., M.T., M.B., S.O. and S.I.; visualization, N.E.H. and A.M.S.; supervision, E.G. and A.B. All authors have read and agreed to the published version of the manuscript.

Funding: This work is financially supported by the Researchers Supporting Project (RSP2024R437). King Saud University, Riyadh, Saudi Arabia.

Data Availability Statement: Data are contained within the article.

Acknowledgments: The authors would like to extend their sincere appreciation to the Researchers Supporting Project, King Saud University, Riyadh, Saudi Arabia, for funding this work through project number (RSP-2024R437).

Conflicts of Interest: The authors declare no conflicts of interest.

References

1. Hao, D.-C.; Xiao, P.-G. Pharmaceutical resource discovery from traditional medicinal plants: Pharmacophylogeny and pharmacophylogenomics. *Chin. Herb. Med.* **2020**, *12*, 104–117. [[CrossRef](#)] [[PubMed](#)]
2. Fabricant, D.S.; Farnsworth, N.R. The value of plants used in traditional medicine for drug discovery. *Environ. Health Perspect.* **2001**, *109* (Suppl. S1), 69–75. [[PubMed](#)]
3. Mohan, S.; Elhassan Taha, M.M.; Makeen, H.A.; Alhazmi, H.A.; Al Bratty, M.; Sultana, S.; Ahsan, W.; Najmi, A.; Khalid, A. Bioactive natural antivirals: An updated review of the available plants and isolated molecules. *Molecules* **2020**, *25*, 4878. [[CrossRef](#)] [[PubMed](#)]
4. Gorlenko, C.L.; Kiselev, H.Y.; Budanova, E.V.; Zamyatnin, A.A., Jr.; Ikryannikova, L.N. Plant secondary metabolites in the battle of drugs and drug-resistant bacteria: New heroes or worse clones of antibiotics? *Antibiotics* **2020**, *9*, 170. [[CrossRef](#)] [[PubMed](#)]
5. Kaoudoune, C.; Benchikh, F.; Benabdallah, H.; Loucif, K.; Mehlous, S.; Amira, S. Gastroprotective effect and in vitro Antioxidant Activities of the Aqueous Extract from *Artemisia absinthium* L. Aerial Parts. *J. Drug Deliv. Ther.* **2020**, *10*, 153–156. [[CrossRef](#)]
6. Ahmad, W.; Hasan, A.; Abdullah, A.; Tarannum, T. Medicinal importance of *Artemisia absinthium* Linn (Afsanteen) in Unani medicine: A review. *Hipp. J. Unani Med.* **2010**, *5*, 117–125.
7. Batiha, G.E.; Olatunde, A.; El-Mleeh, A.; Hetta, H.F.; Al-Rejaie, S.; Alghamdi, S.; Zahoor, M.; Magdy Beshbishy, A.; Murata, T.; Zaragoza-Bastida, A.; et al. Bioactive Compounds, Pharmacological Actions, and Pharmacokinetics of Wormwood (*Artemisia absinthium*). *Antibiotics* **2020**, *9*, 353. [[CrossRef](#)] [[PubMed](#)]
8. Slepetyts, J. Biology and biochemistry of wormwood. VIII. Accumulation dynamics of tannins, ascorbic acid and carotene (Russian). *Труды Академии Наук Литовской Сср Серия С Биологические Науки* **1975**, *1*, 43–48.
9. Canadanovic-Brunet, J.M.; Djilas, S.M.; Cetkovic, G.S.; Tumbas, V.T. Free-radical scavenging activity of wormwood (*Artemisia absinthium* L.) extracts. *J. Sci. Food Agric.* **2005**, *85*, 265–272. [[CrossRef](#)]
10. Akzhigitova, Z.; Baiseitova, A.; Dyusebaeva, M.; Ye, Y.; Jenis, J. Investigation of chemical constituents of *Artemisia absinthium*. *Int. J. Biol. Chem.* **2018**, *11*, 169–177. [[CrossRef](#)]
11. Bhat, R.R.; Rehman, M.U.; Shabir, A.; Mir, M.U.R.; Ahmad, A.; Khan, R.; Masoodi, M.H.; Madkhali, H.; Ganaie, M.A. Chemical composition and biological uses of *Artemisia absinthium* (wormwood). In *Plant and Human Health*; Springer: Berlin/Heidelberg, Germany, 2019; Volume 3, pp. 37–63.

12. Bora, K.S.; Sharma, A. Phytochemical and pharmacological potential of *Artemisia absinthium* Linn. and *Artemisia asiatica* Nakai: A review. *J. Pharm. Res.* **2010**, *3*, 325–328.
13. da Silva, J.A.T. Mining the essential oils of the Anthemideae. *Afr. J. Biotechnol.* **2004**, *3*, 706–720.
14. Picman, A.K. Biological activities of sesquiterpene lactones. *Biochem. Syst. Ecol.* **1986**, *14*, 255–281. [[CrossRef](#)]
15. Wright, C.W. *Artemisia*. medicinal and aromatic plants-Industrial Profiles. *Chapter* **2002**, *1*, 10–22.
16. Ghantous, A.; Gali-Muhtasib, H.; Vuorela, H.; Saliba, N.A.; Darwiche, N. What made sesquiterpene lactones reach cancer clinical trials? *Drug Discov. Today* **2010**, *15*, 668–678. [[CrossRef](#)] [[PubMed](#)]
17. Schmidt, T.J. Structure-activity relationships of sesquiterpene lactones. *Stud. Nat. Prod. Chem.* **2006**, *33*, 309–392.
18. Rodriguez, E.; Towers, G.; Mitchell, J. Biological activities of sesquiterpene lactones. *Phytochemistry* **1976**, *15*, 1573–1580. [[CrossRef](#)]
19. Aberham, A.; Cicek, S.S.; Schneider, P.; Stuppner, H. Analysis of sesquiterpene lactones, lignans, and flavonoids in wormwood (*Artemisia absinthium* L.) using high-performance liquid chromatography (HPLC)—mass spectrometry, reversed phase HPLC, and HPLC—solid phase extraction—nuclear magnetic resonance. *J. Agric. Food Chem.* **2010**, *58*, 10817–10823. [[CrossRef](#)] [[PubMed](#)]
20. Ru, G.; Manns, D.; Wilbert, S. Homoditerpene peroxides from *Artemisia absinthium*. *Phytochemistry* **1992**, *31*, 340–342.
21. Ahamad, J.; Naquvi, K.; Ali, M.; Mir, S. Isoflavone glycosides from aerial parts of *Artemisia absinthium*. *Chem. Nat. Compd.* **2014**, *49*, 996–1000. [[CrossRef](#)]
22. Hbika, A.; Bouyanzer, A.; Saadi, M.; El Ammari, L.; Benali, M.; Majidi, L.; Zarrouk, A. Structural study and thermal stability of Artemetin extracted from *Artemisia absinthium* L. *Chem. Data Collect.* **2022**, *40*, 100880. [[CrossRef](#)]
23. Sridevi, V.K.; Chouhan, H.S.; Singh, N.K.; Singh, S.K. Antioxidant and hepatoprotective effects of ethanol extract of *Vitex glabrata* on carbon tetrachloride-induced liver damage in rats. *Nat. Prod. Res.* **2012**, *26*, 1135–1140. [[CrossRef](#)] [[PubMed](#)]
24. Liu, K.C.-S.C.; Yang, S.-L.; Roberts, M.; Elford, B.; Phillipson, J. Antimalarial activity of *Artemisia annua* flavonoids from whole plants and cell cultures. *Plant Cell Rep.* **1992**, *11*, 637–640. [[CrossRef](#)] [[PubMed](#)]
25. Hu, J.; Ma, W.; Li, N.; Wang, K.-J. Antioxidant and anti-inflammatory flavonoids from the flowers of Chuju, a medical cultivar of *Chrysanthemum morifolium* Ramat. *J. Mex. Chem. Soc.* **2017**, *61*, 282–289. [[CrossRef](#)]
26. Li, W.-X.; Cui, C.-B.; Cai, B.; Wang, H.-Y.; Yao, X.-S. Flavonoids from *Vitex trifolia* L. inhibit cell cycle progression at G2/M phase and induce apoptosis in mammalian cancer cells. *J. Asian Nat. Prod. Res.* **2005**, *7*, 615–626. [[CrossRef](#)] [[PubMed](#)]
27. Talmon, M.; Bosso, L.; Quaregna, M.; Lopatriello, A.; Rossi, S.; Gavioli, D.; Marotta, P.; Caprioglio, D.; Boldorini, R.; Miggiano, R. Anti-inflammatory activity of absinthin and derivatives in human bronchoepithelial cells. *J. Nat. Prod.* **2020**, *83*, 1740–1750. [[CrossRef](#)] [[PubMed](#)]
28. Kasymov, S.Z.; Abdullaev, N.; Sidiyakin, G.; Yagudaev, M. Anabsin—A new diguaianolide from *Artemisia absinthium*. *Chem. Nat. Compd.* **1979**, *15*, 430–435. [[CrossRef](#)]
29. Ortet, R.; Prado, S.; Mouray, E.; Thomas, O.P. Sesquiterpene lactones from the endemic Cape Verdean *Artemisia gorgonum*. *Phytochemistry* **2008**, *69*, 2961–2965. [[CrossRef](#)] [[PubMed](#)]
30. Adekenov, S. Chemical study of *Artemisia austriaca* Jacq. *Int. J. Biol. Chem.* **2021**, *14*, 156–163. [[CrossRef](#)]
31. Bohlmann, F.; Hartono, L.; Jakupovic, J.; Huneck, S. Guaianolides related to arborescin from *Artemisia adamsii*. *Phytochemistry* **1985**, *24*, 1003–1007. [[CrossRef](#)]
32. Hbika, A.; Bouyanzer, A.; Jalal, M.; Setti, N.; Loukili, E.; Aouniti, A.; Kerroum, Y.; Warad, I.; Hammouti, B.; Zarrouk, A.M. The Inhibiting Effect of Aqueous Extracts of *Artemisia absinthium* L. (Wormwood) on the Corrosion of Mild Steel in HCl 1 M. *Anal. Bioanal. Electrochem.* **2023**, *15*, 17–35.
33. Janssens, M.L. Fundamental measurement techniques. In *Flammability Testing of Materials Used in Construction, Transport and Mining*; Elsevier: Amsterdam, The Netherlands, 2022; pp. 23–61.
34. Ma, S.; Chowdhury, S.K.; Alton, K.B. Application of mass spectrometry for metabolite identification. *Curr. Drug Metab.* **2006**, *7*, 503–523. [[CrossRef](#)] [[PubMed](#)]
35. Miceli, N.; Filocamo, A.; Ragusa, S.; Cacciola, F.; Dugo, P.; Mondello, L.; Celano, M.; Maggisano, V.; Taviano, M.F. Chemical characterization and biological activities of phenolic-rich fraction from cauline leaves of *Isatis tinctoria* L. (Brassicaceae) growing in Sicily, Italy. *Chem. Biodivers.* **2017**, *14*, e1700073. [[CrossRef](#)] [[PubMed](#)]
36. Ouahabi, S.; Loukili, E.H.; Daoudi, N.E.; Chebaibi, M.; Ramdani, M.; Rahhou, I.; Bnouham, M.; Fauconnier, M.-L.; Hammouti, B.; Rhazi, L. Study of the Phytochemical Composition, Antioxidant Properties, and In Vitro Anti-Diabetic Efficacy of *Gracilaria bursa-pastoris* Extracts. *Mar. Drugs* **2023**, *21*, 372. [[CrossRef](#)] [[PubMed](#)]
37. Kartal, N.; Sokmen, M.; Tepe, B.; Daferera, D.; Polissiou, M.; Sokmen, A. Investigation of the antioxidant properties of *Ferula orientalis* L. using a suitable extraction procedure. *Food Chem.* **2007**, *100*, 584–589. [[CrossRef](#)]
38. Ouahabi, S.; Loukili, E.H.; Elbouzidi, A.; Taibi, M.; Bouslamti, M.; Nafidi, H.-A.; Salamatullah, A.M.; Saidi, N.; Bellaouchi, R.; Addi, M. Pharmacological properties of chemically characterized extracts from mastic tree: In vitro and in silico assays. *Life* **2023**, *13*, 1393. [[CrossRef](#)]
39. Taibi, M.; Elbouzidi, A.; Ou-Yahia, D.; Dalli, M.; Bellaouchi, R.; Tikent, A.; Roubi, M.; Gseyra, N.; Asehraou, A.; Hano, C. Assessment of the antioxidant and antimicrobial potential of ptychotis verticillata duby essential oil from eastern Morocco: An in vitro and in silico analysis. *Antibiotics* **2023**, *12*, 655. [[CrossRef](#)]
40. Taibi, M.; Elbouzidi, A.; Haddou, M.; Loukili, E.H.; Bellaouchi, R.; Asehraou, A.; Douzi, Y.; Addi, M.; Salamatullah, A.M.; Nafidi, H.-A. Chemical Profiling, Antibacterial Efficacy, and Synergistic Actions of Ptychotis verticillata Duby Essential Oil in Combination with Conventional Antibiotics. *Nat. Prod. Commun.* **2024**, *19*, 1934578X231222785. [[CrossRef](#)]

41. Elbouzidi, A.; Ouassou, H.; Aherkou, M.; Kharchoufa, L.; Meskali, N.; Baraich, A.; Mechchate, H.; Bouhrim, M.; Idir, A.; Hano, C. LC–MS/MS phytochemical profiling, antioxidant activity, and cytotoxicity of the ethanolic extract of *Atriplex halimus* L. against breast cancer cell lines: Computational studies and experimental validation. *Pharmaceuticals* **2022**, *15*, 1156. [[CrossRef](#)] [[PubMed](#)]
42. El Hachlafi, N.; Fikri-Benbrahim, K.; Al-Mijalli, S.H.; Elbouzidi, A.; Jeddi, M.; Abdallah, E.M.; Assaggaf, H.; Bouyahya, A.; Alnasser, S.M.A.; Attar, A. *Tetraclinis articulata* (Vahl) Mast. essential oil as a promising source of bioactive compounds with antimicrobial, antioxidant, anti-inflammatory and dermatoprotective properties: In vitro and in silico evidence. *Heliyon* **2023**, *10*, e23084. [[CrossRef](#)] [[PubMed](#)]
43. Khokra, S.L.; Khan, S.A.; Thakur, P.; Chowdhary, D.; Ahmad, A.; Husain, A. Synthesis, molecular docking and potential antioxidant activity of di/trisubstituted pyridazinone derivatives. *J. Chin. Chem. Soc.* **2016**, *63*, 739–750. [[CrossRef](#)]
44. Khatun, M.C.S.; Muhit, M.A.; Hossain, M.J.; Al-Mansur, M.A.; Rahman, S.A. Isolation of phytochemical constituents from *Stevia rebaudiana* (Bert.) and evaluation of their anticancer, antimicrobial and antioxidant properties via in vitro and in silico approaches. *Heliyon* **2021**, *7*, e08475. [[CrossRef](#)] [[PubMed](#)]
45. Guex, N.; Peitsch, M.C. SWISS-MODEL and the Swiss-Pdb Viewer: An environment for comparative protein modeling. *Electrophoresis* **1997**, *18*, 2714–2723. [[CrossRef](#)] [[PubMed](#)]
46. Pawar, R.P.; Rohane, S.H. Role of autodock vina in PyRx molecular docking. *Asian J. Res. Chem.* **2021**, *5*, 132–134.
47. O’Boyle, N.M.; Banck, M.; James, C.A.; Morley, C.; Vandermeersch, T.; Hutchison, G.R. Open Babel: An open chemical toolbox. *J. Cheminf.* **2011**, *3*, 33. [[CrossRef](#)] [[PubMed](#)]
48. Ferreira, J.F.; Gonzalez, J.M. Analysis of underivatized artemisinin and related sesquiterpene lactones by high-performance liquid chromatography with ultraviolet detection. *Phytochem. Anal.* **2009**, *20*, 91–97. [[CrossRef](#)]
49. Green, M.D.; Mount, D.L.; Wirtz, R.A.; White, N.J. A colorimetric field method to assess the authenticity of drugs sold as the antimalarial artesunate. *J. Pharm. Biomed. Anal.* **2000**, *24*, 65–70. [[CrossRef](#)] [[PubMed](#)]
50. Christen, P.; Veuthey, J. New trends in extraction, identification and quantification of artemisinin and its derivatives. *Curr. Med. Chem.* **2001**, *8*, 1827–1839. [[CrossRef](#)] [[PubMed](#)]
51. Ivanescu, B.; Miron, A.; Corciova, A. Sesquiterpene lactones from Artemisia genus: Biological activities and methods of analysis. *J. Anal. Methods Chem.* **2015**, *2015*, 247685. [[CrossRef](#)] [[PubMed](#)]
52. Arjunan, V.; Devi, L.; Subbalakshmi, R.; Rani, T.; Mohan, S. Synthesis, vibrational, NMR, quantum chemical and structure-activity relation studies of 2-hydroxy-4-methoxyacetophenone. *Spectrochim. Acta Part A Mol. Biomol. Spectrosc.* **2014**, *130*, 164–177. [[CrossRef](#)] [[PubMed](#)]
53. El-Gammal, O.; Rakha, T.; Metwally, H.; El-Reash, G.A. Synthesis, characterization, DFT and biological studies of isatinpicolinohydrazone and its Zn (II), Cd (II) and Hg (II) complexes. *Spectrochim. Acta Part A Mol. Biomol. Spectrosc.* **2014**, *127*, 144–156. [[CrossRef](#)] [[PubMed](#)]
54. Regti, A.; El Ayouchia, H.B.; Laamari, M.R.; Stiriba, S.E.; Anane, H.; El Haddad, M. Experimental and theoretical study using DFT method for the competitive adsorption of two cationic dyes from wastewaters. *Appl. Surf. Sci.* **2016**, *390*, 311–319. [[CrossRef](#)]
55. Choudhary, V.; Bhatt, A.; Dash, D.; Sharma, N. DFT calculations on molecular structures, HOMO–LUMO study, reactivity descriptors and spectral analyses of newly synthesized diorganotin (IV) 2-chloridophenylacetohydroxamate complexes. *J. Comput. Chem.* **2019**, *40*, 2354–2363. [[CrossRef](#)] [[PubMed](#)]
56. Tzanova, M.; Grozeva, N.; Gerdzhikova, M.; Argirova, M.; Pavlov, D.; Terzieva, S. Flavonoid content and antioxidant activity of *Betonica bulgarica* Degen et Neič. *Bulg. Chem. Commun.* **2018**, *50*, 90–97.
57. Benchikh, F.; Amira, S.; Benabdallah, H. The evaluation of antioxidant capacity of different fractions of *Myrtus communis* L. leaves. *Annu. Res. Rev. Biol.* **2018**, *22*, 1–14. [[CrossRef](#)]
58. Martins, A.; Mignon, R.; Bastos, M.; Batista, D.; Neng, N.R.; Nogueira, J.M.; Vizetto-Duarte, C.; Custódio, L.; Varela, J.; Rauter, A.P. In vitro antitumoral activity of compounds isolated from *Artemisia gorgonum* Webb. *Phytother. Res.* **2014**, *28*, 1329–1334. [[CrossRef](#)] [[PubMed](#)]
59. Elbouzidi, A.; Taibi, M.; Laaraj, S.; Loukili, E.H.; Haddou, M.; El Hachlafi, N.; Naceiri Mrabti, H.; Baraich, A.; Bellaouchi, R.; Asehraou, A. Chemical profiling of volatile compounds of the essential oil of grey-leaved rockrose (*Cistus albidus* L.) and its antioxidant, anti-inflammatory, antibacterial, antifungal, and anticancer activity in vitro and in silico. *Front. Chem.* **2024**, *12*, 1334028. [[CrossRef](#)] [[PubMed](#)]
60. Harrison, R. Structure and function of xanthine oxidoreductase: Where are we now? *Free Radic. Biol. Med.* **2002**, *33*, 774–797. [[CrossRef](#)] [[PubMed](#)]
61. Harrison, R. Physiological roles of xanthine oxidoreductase. *Drug Metab. Rev.* **2004**, *36*, 363–375. [[CrossRef](#)] [[PubMed](#)]
62. Scherz-Shouval, R.; Elazar, Z. Regulation of autophagy by ROS: Physiology and pathology. *Trends Biochem. Sci.* **2011**, *36*, 30–38. [[CrossRef](#)] [[PubMed](#)]
63. Juan, C.A.; Pérez de la Lastra, J.M.; Plou, F.J.; Pérez-Lebeña, E. The chemistry of reactive oxygen species (ROS) revisited: Outlining their role in biological macromolecules (DNA, lipids and proteins) and induced pathologies. *Int. J. Mol. Sci.* **2021**, *22*, 4642. [[CrossRef](#)]
64. Vickneson, K.; George, J. Xanthine oxidoreductase inhibitors. In *Reactive Oxygen Species: Network Pharmacology and Therapeutic Applications*; Springer: Berlin/Heidelberg, Germany, 2021; pp. 205–228.
65. Andrews, B.A.; Dyer, R.B. Comparison of the Role of Protein Dynamics in Catalysis by Dihydrofolate Reductase from *E. coli* and *H. sapiens*. *J. Phys. Chem. B* **2022**, *126*, 7126–7134. [[CrossRef](#)] [[PubMed](#)]

66. Chawla, P.; Teli, G.; Gill, R.K.; Narang, R.K. An insight into synthetic strategies and recent developments of dihydrofolate reductase inhibitors. *ChemistrySelect* **2021**, *6*, 12101–12145. [[CrossRef](#)]
67. Bhagat, K.; Kumar, N.; Kaur Gulati, H.; Sharma, A.; Kaur, A.; Singh, J.V.; Singh, H.; Bedi, P.M.S. Dihydrofolate reductase inhibitors: Patent landscape and phases of clinical development (2001–2021). *Expert Opin. Ther. Pat.* **2022**, *32*, 1079–1095. [[CrossRef](#)] [[PubMed](#)]
68. Bhabha, G.; Ekiert, D.C.; Jennewein, M.; Zmasek, C.M.; Tuttle, L.M.; Kroon, G.; Dyson, H.J.; Godzik, A.; Wilson, I.A.; Wright, P.E. Divergent evolution of protein conformational dynamics in dihydrofolate reductase. *Nat. Struct. Mol. Biol.* **2013**, *20*, 1243–1249. [[CrossRef](#)] [[PubMed](#)]
69. Wróbel, A.; Arciszewska, K.; Maliszewski, D.; Drozdowska, D. Trimethoprim and other nonclassical antifolates an excellent template for searching modifications of dihydrofolate reductase enzyme inhibitors. *J. Antibiot.* **2020**, *73*, 5–27. [[CrossRef](#)] [[PubMed](#)]
70. Bayazeed, A.; Alenazi, N.A.; Alsaedi, A.M.; Ibrahim, M.H.; Al-Qurashi, N.T.; Farghaly, T.A. Formazan analogous: Synthesis, antimicrobial activity, dihydrofolate reductase inhibitors and docking study. *J. Mol. Struct.* **2022**, *1258*, 132653. [[CrossRef](#)]
71. Moujir, L.; Callies, O.; Sousa, P.M.; Sharopov, F.; Seca, A.M. Applications of sesquiterpene lactones: A review of some potential success cases. *Appl. Sci.* **2020**, *10*, 3001. [[CrossRef](#)]
72. Lai, H.C.; Singh, N.P.; Sasaki, T. Development of artemisinin compounds for cancer treatment. *Investig. New Drugs* **2013**, *31*, 230–246. [[CrossRef](#)] [[PubMed](#)]
73. White, N.J. Qinghaosu (artemisinin): The price of success. *Science* **2008**, *320*, 330–334. [[CrossRef](#)] [[PubMed](#)]
74. Stavrianidi, A. A classification of liquid chromatography mass spectrometry techniques for evaluation of chemical composition and quality control of traditional medicines. *J. Chromatogr. A* **2020**, *1609*, 460501. [[CrossRef](#)]
75. Beer, M.F.; Bivona, A.E.; Sánchez Alberti, A.; Cerny, N.; Reta, G.F.; Martín, V.S.; Padrón, J.M.; Malchiodi, E.L.; Sülsen, V.P.; Donadel, O.J. Preparation of sesquiterpene lactone derivatives: Cytotoxic activity and selectivity of action. *Molecules* **2019**, *24*, 1113. [[CrossRef](#)] [[PubMed](#)]
76. Sokovic, M.; Ciric, A.; Glamoclija, J.; Skaltsa, H. Biological activities of sesquiterpene lactones isolated from the genus *Centaurea* L. (Asteraceae). *Curr. Pharm. Des.* **2017**, *23*, 2767–2786. [[CrossRef](#)] [[PubMed](#)]
77. Ma, C.; Meng, C.-W.; Zhou, Q.-M.; Peng, C.; Liu, F.; Zhang, J.-W.; Zhou, F.; Xiong, L. New sesquiterpenoids from the stems of *Dendrobium nobile* and their neuroprotective activities. *Fitoterapia* **2019**, *138*, 104351. [[CrossRef](#)] [[PubMed](#)]
78. Cheriti, A.; Belboukhari, N. *Terpenoids of the Saharan Medicinal Plants Launaea Cass. Genus (Asteraceae) and Their Biological Activities*; Nova Science Publishers Inc.: New York, NY, USA, 2015; pp. 51–70.
79. Li, Q.; Wang, Z.; Xie, Y.; Hu, H. Antitumor activity and mechanism of costunolide and dehydrocostus lactone: Two natural sesquiterpene lactones from the Asteraceae family. *Biomed. Pharmacother.* **2020**, *125*, 109955. [[CrossRef](#)] [[PubMed](#)]
80. Pandey, M.M.; Rastogi, S.; Rawat, A.K.S. *Saussurea costus*: Botanical, chemical and pharmacological review of an ayurvedic medicinal plant. *J. Ethnopharmacol.* **2007**, *110*, 379–390. [[CrossRef](#)] [[PubMed](#)]
81. Kim, D.Y.; Choi, B.Y. Costunolide—A bioactive sesquiterpene lactone with diverse therapeutic potential. *Int. J. Mol. Sci.* **2019**, *20*, 2926. [[CrossRef](#)]
82. Lin, X.; Peng, Z.; Su, C. Potential anti-cancer activities and mechanisms of costunolide and dehydrocostuslactone. *Int. J. Mol. Sci.* **2015**, *16*, 10888–10906. [[CrossRef](#)] [[PubMed](#)]
83. Wang, J.; Su, S.; Zhang, S.; Zhai, S.; Sheng, R.; Wu, W.; Guo, R. Structure-activity relationship and synthetic methodologies of α -santonin derivatives with diverse bioactivities: A mini-review. *Eur. J. Med. Chem.* **2019**, *175*, 215–233. [[CrossRef](#)] [[PubMed](#)]

Disclaimer/Publisher’s Note: The statements, opinions and data contained in all publications are solely those of the individual author(s) and contributor(s) and not of MDPI and/or the editor(s). MDPI and/or the editor(s) disclaim responsibility for any injury to people or property resulting from any ideas, methods, instructions or products referred to in the content.